Loss of Flexibility in Geosynthetics Subjected to Chemical Exposure: Experiments, Constitutive Models and Computations and Estimates for Contaminant Leakage

A. P.S. Selvadurai[1]
[1]*Department of Civil Engineering and Applied Mechanics, McGill University, Montreal, QC, Canada H3A 0C3*
E-mail: patrick.selvadurai@mcgill.ca

ABSTRACT: The paper presents results of recent research related to the development of advanced mathematical models for describing the behaviour of strain rate sensitive materials such as geosynthetics that are used extensively as barriers to the migration of contaminants and other hazardous materials. The important finding of the research is that the leaching of the plasticizer from the geosynthetic can lead to a loss of hyperelasticity of the material, which is a key functional requirement for a geosynthetic. It is also shown that constitutive models can be developed to describe the mechanical behaviour of the geosynthetic in its virgin state and upon direct exposure to pure ethanol for thirteen months. A computational approach is used to evaluate the results of separate laboratory experiments involving transverse indentation of geosynthetic membranes that are fixed along a circular boundary and tested in either its untreated state or after prolonged exposure to ethanol.

KEYWORDS: Geosynthetics, Loss of plasticizer, Constitutive modelling, Membrane indentation tests, Computational modelling

1. INTRODUCTION

Polyvinyl chloride (PVC) membranes, also referred to as geosynthetics or geomembranes, are used quite extensively in geoenvironmental endeavors in order to prevent groundwater contamination due to leakage of leachates from landfill and from hazardous waste sites such as mine tailings ponds. The earliest known use of geosynthetic membranes for environmental protection is not well documented. In terms of waterproofing of dams (Cazzuffi, 1987) and upstream control from seepage in clay (Terzaghi and Lacroix, 1964) the usage dates back to the 1950's. In terms of its use in the landfill industry, the applications generally date to the early 1980's. The applications as one of the barriers for preventing leakage of contaminants from landfill is extensive and no attempt will be made to provide a comprehensive bibliography that can be found in conference proceedings, texts and review articles (Koerner, 1998; Zornberg and Christopher, 1999; Rowe and Sangam, 2002; Bouazza et al., 2002; Yu and Selvadurai, 2005). PVC membranes continue to promoted as an important component of multi-barrier containment systems that also consist of alternate layers of impermeable clay and leachate collection systems. The use of geosynthetic membranes used as landfill liners has no stated accountability for longevity. Geosynthetic being a manufactured material has, by definition, a finite life. A landfill on the other hand is expected to have a significantly longer life in terms of its pollution and contamination potential. This presents a dilemma in terms of what is the purpose and useful life expectancy of a manufactured barrier in a waste containment setting. Even prior to the start of its function as a waste containment barrier, geosynthetic liners can be subjected to a number of adverse effects. (i) Exposure of the geosynthetic to ultraviolet light during its installation is recognized as a source that can introduce non-uniform degradation. Although chemical additives can be incorporated to minimize the degradation, the overall effectiveness cannot be gauged with certainty. (ii) Geosynthetic liners are supplied in rolls and welded or bonded in place at the joints. The welding or bonding action can introduce heterogeneity in strength, stiffness and the polymeric structure of the geosynthetic. In the event of excessive deformation of the soils beneath the landfill and the anchoring of the geosynthetic in zones, the heterogeneous regions can act as stress raisers that can lead to the premature malfunction of the liner. (iii) In the event of interaction of leachate containing chemicals with the geosynthetic, the leaching of the plasticizer can lead to loss of its flexibility, which can be detrimental to the expected retaining capabilities of the geosynthetic liner. (iv) If the geosynthetic liner degrades, this will create a weak barrier or a conduit that can facilitate contaminant movement and depending on the configuration of the multi-barrier system, will promote enhanced leakage or diffusion of chemicals to the subsoils.

A primary requirement of a geosynthetic relates to its ability to undergo large deformations and to maintain its integrity, thereby impeding the migration of hazardous chemicals and contaminants to the environment. Experiments conducted in connection with this research indicate that the interaction of the geosynthetic with relatively commonly occurring chemicals in landfill environments such as acetone and ethanol leads to the loss of plasticizers that contribute to the hyperelasticity of the material. The flexibility of a geosynthetic is derived largely from plasticizers incorporated into its chemical composition. Recent research has shown that the exposure of the geosynthetic membranes to chemicals such as acetone and ethanol can lead to embrittlement of the membrane as a result of the leaching of the plasticizer. The longevity of the containment provided by PVC geosynthetics can be influenced by these factors, specifically in situations involving the thermal desiccation of clay. Desiccation cracking can be caused by moisture depletion in the clay barrier following exothermic processes associated with the decay of organic matter in the landfill. A cracked clay barrier provides a pathway for contaminants to come into direct contact with a geosynthetic barrier. The direct exposure of the plasticized PVC membrane to chemical action is a problem of major concern. The exposure of the PVC to chemicals can result in mechanical alterations in the material, largely as a result of leaching of the plasticizer**,** which contributes to the flexibility of the PVC (Pita et al., 2002). Exposure to commonly occurring chemicals such as acetone and ethanol can lead to a loss of hyperelasticity in the geosynthetics (Haedrich, 1995; Contamin and DeBeauvais, 1998).

2. EXPERIMENTS

Uniaxial experiments (Figure 1) conducted in connection with this research also show an alteration in the mechanical properties of a PVC membranes during exposure to pure ethanol. These alterations include a progressive loss of large strain flexibility, embrittlement, the development of a distinct initial linear elastic modulus and the development of a yield point (Figure 2). The initial linear elastic modulus and the yield stress of the material continuously increase over an exposure period of 2 months after which there is a slight decrease in the peak yield value, which remains unaltered during further exposure.

The rapid alteration in the mechanical properties of the geosynthetic membrane in the first two months correlates well with the X-Ray fluorescence evidence, which also indicates a loss of plasticizer during this period. The plasticizer content is identified through the weight ratio $R_{O/Cl}$ of the oxygen element and chloride element in the geosynthetic specimen that has been originally plasticized with 25%-35% weight content of a phthalate plasticizer.

The loss of plasticizer after a two-month exposure to pure ethanol leads to (i) a reduction in the flexibility of the geosynthetic, (ii) an increase in the failure stress and (iii) the development of a strain-hardening regime in the stress-strain response (Figure 2).

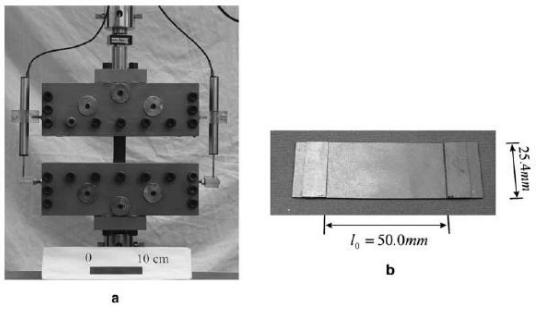

Figure 1 Uniaxial testing of specimens of PVC membranes

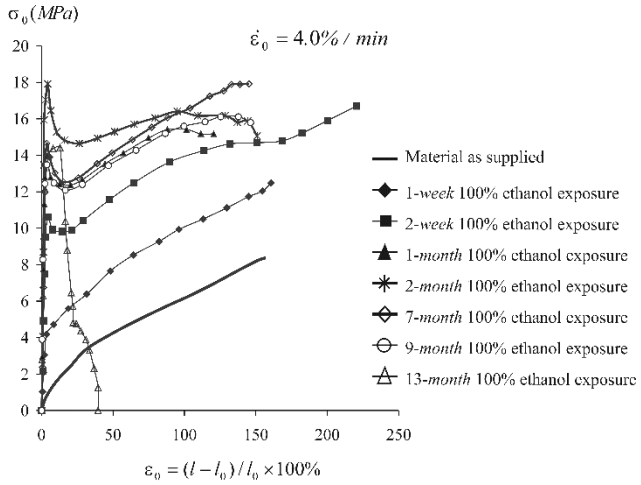

Figure 2 Behaviour of PVC specimens during exposure to pure ethanol

For PVC geosynthetics that have been exposed to ethanol for a period of 13 months, the stress-strain behaviour of the specimen exhibits a mechanical response similar to a PVC material containing a very low content of DOP (Dioctyl phthalate) plasticizer (less than 15%) (Pita et al., 2002). With significant loss of plasticizer from the specimen, the PVC geosynthetic subjected to a 13 month chemical exposure shows only moderate deformability with a failure strain of about 20%. For a specimen that is loaded at a lower strain-rate (e.g. $0.05\,\mathrm{min}^{-1}$), however, the large strain deformability of a PVC material with a low content of plasticizer can be recovered (Pezzin et al., 1972). The results of the computational simulations are compared with the experimental results. We observe that the constitutive models that use a basic hyperelastic constitutive relationship of the Mooney-Rivlin form, where the parameters are strain rate- and chemical exposure-dependent, provides a convenient model for the examination of the constitutive behaviour of a geosynthetic both in its untreated state and after prolonged exposure to ethanol. The exposure of the geosynthetic membrane to pure ethanol is intended to model an extreme condition. Ethanol is a hydrocarbon that is used quite extensively in automobiles and containers of ethanol can be disposed of either accidentally or deliberately in landfill. The direct contact between the ethanol and the geosynthetic membrane can result from desiccation cracking of the clay liners that are intended to provide additional protection to the geosynthetic barrier.

3. CONSTITUTIVE MODELLING

Purely hyperelastic rubber-like materials exhibit virtually no irreversible phenomena in terms of permanent deformations and energy dissipation during quasi-static load cycling (Treloar, 1943; Rivlin, 1948; Green and Adkins, 1970; Spencer, 1970; Selvadurai, 2002; Selvadurai and Suvorov, 2016). In contrast, glassy polymeric materials exhibit appreciable irreversible effects including development of permanent strains during loading-unloading cycles and strain-rate effects (Sweeny and Ward, 1995). The constitutive modelling of such materials can be approached at a variety of levels ranging from elementary power law creep models to generalized continuum models applicable to non-linear viscoelastic materials. The This paper presents constitutive models that first describe the hyperelastic behaviour of a geosynthetic material in its as supplied condition. The modelling accounts for both reversible and irreversible components of hyperelastic behaviour and incorporates strain rate dependency in the constitutive response. The constitutive modelling is then extended to include the loss of hyperelasticity as a result of exposure to pure ethanol. The constitutive parameters were determined from uniaxial tests and constrained tests conducted at different strain rates. The constitutive models were implemented in a general purpose finite element code to examine the mechanics of a membrane fixed along a circular boundary and loaded by a hemi-spherical indenter. Chemical action on these materials is to leach out the plasticizer that provides large strain capability without initiation of fracture and/or damage. This paper presents the results of experiments conducted on PVC in its as supplied state and subjected to chemical treatment, in order to determine the constitutive relationships that govern hyperelastic behaviour as well as loss of hyperelasticity resulting from chemical action (Selvadurai and Yu (2006 a,b, 2008; Yu and Selvadurai, 2005, 2007). The constitutive models developed, take into consideration strain-rate sensitivity and large strain effects in the untreated material and distinct yield and strain-rate sensitivity in the chemically treated material. The modelling uses forms of constitutive potentials that are derived from hyperelastic rubberlike materials undergoing moderately large strains. We consider the deformation such that the position of a generic particle in the deformed configuration is denoted by $x_i\ (i = 1,2,3)$ and the coordinates of the same particle in the reference configuration are denoted by $X_A\ (A = 1,2,3)$. Restricting attention to incompressible materials (for which $\det \mathbf{F} = 1$), the deformation gradient tensor is given by

$$\mathbf{F} = \left\| \partial x_i / \partial X_A \right\| \tag{1}$$

As suggested by Lee (1969) and others, the total deformation gradient tensor $\mathbf{F}$ can be decomposed into its elastic (*e*) and irreversible (*u*) components, i.e.

$$\mathbf{F} = \mathbf{F}^e \mathbf{F}^u \tag{2}$$

Strain tensors in terms of $\mathbf{B}^e$ and $\mathbf{B}^u$ are defined by

$$\mathbf{B}^e = \mathbf{F}^e (\mathbf{F}^e)^T \ ; \ \mathbf{B}^u = \mathbf{F}^u (\mathbf{F}^u)^T \tag{3}$$

and the strain-rate is defined (Spencer, 2004) by

$$\begin{aligned} &\mathbf{L} = \dot{\mathbf{F}}\mathbf{F}^{-1} = \mathbf{D} + \mathbf{W} = \dot{\mathbf{F}}^e (\mathbf{F}^e)^{-1} + \mathbf{F}^e [\dot{\mathbf{F}}^u (\mathbf{F}^u)^{-1}](\mathbf{F}^e)^{-1} \\ &\mathbf{L}^u = \dot{\mathbf{F}}^u (\mathbf{F}^u)^{-1} \quad ; \quad \mathbf{D}^u = \frac{1}{2}[\mathbf{L}^u + (\mathbf{L}^u)^T] \end{aligned} \tag{4}$$

The invariants of $\mathbf{B}^e$, $\mathbf{B}^u$ are

$$I_1^h = (\lambda_1^h)^2 + (\lambda_2^h)^2 + (\lambda_3^h)^2$$
$$I_2^h = \frac{1}{(\lambda_1^h)^2} + \frac{1}{(\lambda_2^h)^2} + \frac{1}{(\lambda_3^h)^2} \qquad (5)$$
$$I_3^h = \lambda_1^h \lambda_2^h \lambda_3^h = 1; (h = e,u)$$

and λ_i^e and λ_i^u $(i = 1,2,3)$ are, respectively, the principal stretches of the elastic and irreversible components. In this research, the general constitutive model for both the untreated and chemically treated PVC has been selected to conform to a single generic form (Figure 3). The large elastic deformation can be modelled through the introduction of a strain energy function W^e (component *C*) of a modified Mooney-Rivlin form, which is considered to be a satisfactory form of a strain energy function for hyperelastic materials that experience moderately large strains (Spencer, 2004; Mooney, 1940; Rivlin 1960; Selvadurai and Spencer, 1972; Selvadurai, 1974, 1975, 2006; Selvadurai et al, 1988; Selvadurai and Shi, 2012; Selvadurai and Yu, 2005; Selvadurai and Suvorov, 2016, 2017; Suvorov and Selvadurai, 2016).

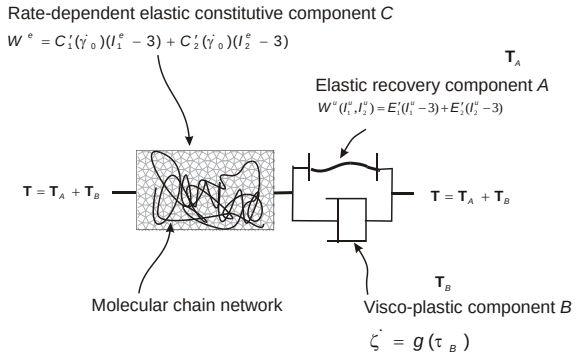

Figure 3 Schematic representation of the constitutive components

In the model proposed, the irreversible deformation can be characterized by a visco-plastic model, which can be visualized as consisting of an elastic component *A* of the finite strain contributing to the elastic recovery, in parallel with a visco-plastic component *B* that accounts for the rate-dependent effects during unloading. The finite strain component *A*, which is similar to component *C*, can be characterized by a strain energy function W^u of the Mooney-Rivlin form.

The component *C* is sufficient to characterize the constitutive behaviour of an untreated material during monotonic loading without unloading or a chemically treated material experiencing strains prior to the yield point. In this case, there are no irreversible effects and the total deformation gradient $\mathbf{F}$ is the same as the elastic deformation gradient $\mathbf{F}^e$.

The stress $\mathbf{T}_C$ associated with the component *C*, which is the total Cauchy stress $\mathbf{T}$ of the untreated or chemically treated material, is an isotropic function of elastic strain tensor $\mathbf{B}^e$ and takes the form

$$\mathbf{T} = \mathbf{T}_C = -\tilde{p}^e \mathbf{I} + \psi_1^e \mathbf{B}^e + \psi_2^e \left(\mathbf{B}^e\right)^2$$
$$\psi_1^e = 2\left(\frac{\partial W^e}{\partial I_1^e} + I_1^e \frac{\partial W^e}{\partial I_2^e}\right); \quad \psi_2^e = -2\frac{\partial W^e}{\partial I_2^e} \qquad (6)$$

where $\tilde{p}^e$ is a scalar pressure. Following the approach proposed by Sweeny and Ward (1995) to account for the influence of the strain rate on the strain energy function, we adopt the following type of strain energy function for the untreated material:

$$W^e(I_1^e, I_2^e) = C_1'(I_1^e - 3) + C_2'(I_2^e - 3) \qquad (7)$$

where

$$C_1' = C_1 + \begin{cases} \kappa_1 ln\left(|\dot{\gamma}_0| / \dot{\gamma}_c\right); & (|\dot{\gamma}_0| \geq \dot{\gamma}_c) \\ 0 \quad ; & (|\dot{\gamma}_0| < \dot{\gamma}_c) \end{cases}$$
$$C_2' = C_2 + \begin{cases} \kappa_2 ln\left(|\dot{\gamma}_0| / \dot{\gamma}_c\right); & (|\dot{\gamma}_0| \geq \dot{\gamma}_c) \\ 0 \quad ; & (|\dot{\gamma}_0| \geq \dot{\gamma}_c) \end{cases} \qquad (8)$$

In (8), $\dot{\gamma}_0$ is a generalized form of a combined stretch-rate that depends only on the in-plane principal stretches λ_i $(i = 1,2)$, such that

$$\dot{\gamma}_0 = \frac{d\gamma_0}{dt} \quad ; \quad \gamma_0 = [(\bar{\lambda}_1 - 1)^\alpha + (\bar{\lambda}_2 - 1)^\alpha]^{1/\alpha} \qquad (9)$$

where, $\bar{\lambda}_i$ have a conditional dependence on the total principal stretches λ_i to take into consideration either the stretching or the unloading response: i.e.

$$\bar{\lambda}_i = \begin{cases} \lambda_i \quad ; \quad (\lambda_i \geq 1) \quad ; \quad i = (1,2) \\ 1 \quad ; \quad (\lambda_i < 1) \quad ; \quad i = (1,2) \end{cases} \qquad (10)$$

and α is a material (combination) parameter. When the geosynthetics specimen is subjected to a uniaxial stretch, the principal stretches in the other directions are less than unity and therefore the definition of γ_0 reduces to that of the uniaxial strain ε_0 . In (8), C_1' and C_2' are the modified Mooney-Rivlin parameters, κ_1 and κ_2 are parameters that define the strain-rate sensitivity and $\dot{\gamma}_c$ is defined as the rate-independent threshold strain-rate. At loading rates $|\dot{\gamma}_0| \leq \dot{\gamma}_c$, the strain-rate effects are disregarded. For a chemically treated material, a classical Hookean isotropic incompressible elastic model, without the consideration of large strain effects, can adequately describe its initial elastic behaviour prior to the yield point. To conform to the description of the model for the *untreated* material, we adopt a neo-Hookean form of the strain energy function, which can be derived from a Mooney-Rivlin form of strain energy function (7) with C_2' independent of the strain-rate and always equal to zero. When examining the untreated material during unloading or the chemically-treated material experiencing strains beyond the yield point, permanent strains ensue. Therefore, the additional visco-plastic model characterized by an elastic recovery component *A* in parallel to a visco-plastic component *B* should be added in series to the component *C*. The component *A* is described by a further conventional finite strain approach with a strain energy function W^u of a Mooney-Rivlin form:

$$\mathbf{T}_A = -\tilde{p}^u\mathbf{I} + \psi_1^u\mathbf{B}^u + \psi_2^u(\mathbf{B}^u)^2$$
$$\psi_1^u = 2\left(\frac{\partial W^u}{\partial I_1^u} + I_1^u\frac{\partial W^u}{\partial I_2^u}\right); \quad \psi_2^u = -2\frac{\partial W^u}{\partial I_2^u} \tag{11}$$

where $\tilde{p}^u$ is a scalar pressure and

$$W^u(I_1^u, I_2^u) = E_1'(I_1^u - 3) + E_2'(I_2^u - 3) \tag{12}$$

In (12), E_1' has the conditional constraint for an untreated material: i.e.

$$E_1' = \begin{cases} \to\infty; & (\dot{\gamma}_0 \geq -\dot{\gamma}_c^v) \\ 0 \quad ; & (\dot{\gamma}_0 < -\dot{\gamma}_c^v) \end{cases} \tag{13}$$

and E_2' is a constant. The choice of E_1' in (13) is intended to take into account the non-symmetric behaviour of the elastic recovery component *A* during the loading-unloading response, where, at the loading stage, $\dot{\gamma}_0 \geq 0$, and at the extremely low loading rate $|\dot{\gamma}_0| \leq \dot{\gamma}_c^v$ (where $\dot{\gamma}_c^v$ *is* the viscous threshold strain-rate). The visco-plastic deformation that applies to components *A* and *B* is restricted due to the choice of an infinite value for E_1'. As a result, only the elastic deformation of component *C* is applicable for the untreated material. Upon unloading, however, the visco-plastic deformation is fully released due to the zero value of E_1' chosen in (13). All three components *A*, *B* and *C* take effect during the unloading of the untreated material. For a chemically treated specimen, E_1' must also take into consideration the yield of the material and has the form

$$\begin{aligned} &E_1' \to \infty \quad ; \quad \dot{\gamma}_0 \geq -\dot{\gamma}_c^v \quad \text{and} \quad \gamma_0 \leq \zeta_y \\ &E_1' = E_y' \quad ; \quad \dot{\gamma}_0 \geq -\dot{\gamma}_c^v \quad \text{and} \quad \gamma_0 > \zeta_y \\ &E_1' = 0 \quad ; \quad \dot{\gamma}_0 < -\dot{\gamma}_c^v \end{aligned} \tag{14}$$

where ζ_y is the yield strain and E_y' is the post-yield hardening modulus. Prior to the yield point, the visco-plastic deformation is restricted; beyond the yield point, however, the visco-plastic deformation is released due to the finite value of E_y'. This leads to the deviation of the material behaviour from an initial linear elastic behaviour to a softening behaviour followed by hardening behaviour at larger strains. The possibility of rate-dependency of the hardening modulus E_y' is also considered; i.e.

$$E_y' = E_y + \begin{cases} \kappa_y \ln\left(|\dot{\gamma}_0| / \dot{\gamma}_c^v\right) & ; \quad (|\dot{\gamma}_0| \geq \dot{\gamma}_c^v) \\ 0 & ; \quad (|\dot{\gamma}_0| < \dot{\gamma}_c^v) \end{cases} \tag{15}$$

where κ_y is the rate sensitivity, E_y is the rate-independent hardening modulus, and, at $|\dot{\gamma}_0| \leq \dot{\gamma}_c^v$, the viscous effect is omitted.

The stress $\mathbf{T}_B$ in component *B* is defined in terms of the finite plastic strain-rate $\mathbf{D}^u$, which is assumed to be related to the deviatoric component of the normalized effective stress tensor $\mathbf{N}_B$. In the component *B*, the visco-plastic effects are modelled through a relationship of the form

$$\mathbf{D}^u = \dot{\zeta}\,\mathbf{N}_B; \quad \mathbf{N}_B = \frac{1}{\sqrt{2}\tau_B}\mathbf{T}_B'; \quad \tau_B = \left\{\frac{1}{2}tr\left[\left(\mathbf{T}_e'\right)^2\right]\right\}^{1/2} \tag{16}$$

and $\mathbf{T}_B'$ is the deviatoric component of the Cauchy stress tensor $\mathbf{T}_B$ applicable to visco-plastic phenomena, as depicted in Figure 2. Also, in (16) the visco-plastic strain-rate $\dot{\zeta}$ is generally assumed to be a function of the effective stress τ_B and the strain-rate $\dot{\gamma}_0$, i.e.

$$\dot{\zeta} = \left(\frac{\tau_B}{q}\right)^{1-s}|\dot{\gamma}_0|\begin{cases} \dfrac{1}{\left(|\dot{\gamma}_0| / \gamma_c^v\right)^s} & ; \quad (|\dot{\gamma}_0| \geq \dot{\gamma}_c^v) \\ 1 & ; \quad (|\dot{\gamma}_0| < \dot{\gamma}_c^v) \end{cases} \tag{17}$$

In (17), s is the viscous sensitivity to the rate effect. Also at extremely low loading rates $|\dot{\gamma}_0| \leq \dot{\gamma}_c^v$, the dependency of $\dot{\zeta}$ on the strain-rate γ_0 is neglected; therefore, the parameter q can be interpreted as the static yielding stress of the material. It should also be noted that when $s \approx 0$, the value of $\dot{\gamma}_c^v$ is inapplicable and the response of the material reduces to a pure plastic response.

The stress states in the elastic recovery responses, denoted by $\mathbf{T}_A$ and the visco-plastic responses, denoted by $\mathbf{T}_B$, are added to generate the Cauchy stress: i.e.

$$\mathbf{T} = \mathbf{T}_C = \mathbf{T}_A + \mathbf{T}_B \tag{18}$$

In summary, a single generalized form of a constitutive model intended for describing large strain hyperelastic behaviour, strain-rate effects and moderately large irreversible plastic strains has been adopted for modelling both the untreated and chemically treated materials. The mechanical response of the untreated material, however, has to distinguish between loading and unloading through a selective treatment of the elastic parameter of the elastic recovery component. During loading, the visco-plastic deformation of the untreated material is restricted and the only deformation is attributed to elastic effects; upon unloading, however, the visco-plastic component is fully released and the unloading behaviour is accompanied by irreversible deformations. For the chemically-treated material, the material responses also have to take into account the yield point. Prior to yield, the visco-plastic deformation is restricted; beyond the yield point, however, the visco-plastic component is released, which accounts for further softening and hardening behaviour. The equations used to describe the general form of the constitutive model for both the untreated and chemically-treated material, can be summarized as follows:

Constitutive Equations used for modelling the Untreated Material

Loading:

Deformation Gradient: $\mathbf{F} = \mathbf{F}^e$

Component *A* ($\mathbf{T}_A$): Deformation restricted

Component *B* ($\mathbf{T}_B$): Deformation restricted

Component *C* ($\mathbf{T}_C$): Eq. (6), (7), (8), (9), (10)

Unloading:

Deformation Gradient: $\mathbf{F} = \mathbf{F}^e\mathbf{F}^u$

Component *A* ($\mathbf{T}_A$): Eq. (11), (12) with $E_1' = 0$

Component *B* ($\mathbf{T}_B$): Eq. (16), (17)

Component *C* ($\mathbf{T}_C$): Eq. (6), (7), (8), (9), (10)

Constitutive Equations used for modelling the Chemically Treated Material

Loading prior to Yield Point:

Deformation Gradient: $\mathbf{F} = \mathbf{F}^e$

Component *A* ($\mathbf{T}_A$): Deformation restricted

Component *B* ($\mathbf{T}_B$): Deformation restricted

Component *C* ($\mathbf{T}_C$): Eq. (6) with $C_2' = 0$, (7), (8), (9), (10)

Loading beyond Yield Point:

Deformation Gradient: $\mathbf{F} = \mathbf{F}^e\mathbf{F}^u$

Component *A* ($\mathbf{T}_A$): Eq. (11), (12) with $E_1' = E_y'$, and (15)

Component *B* ($\mathbf{T}_B$): Eq. (16), (17)

Component *C* ($\mathbf{T}_C$): Eq. (6) with $C_2' = 0$,(7), (8), (9), (10)

Unloading:

Deformation Gradient: $\mathbf{F} = \mathbf{F}^e\mathbf{F}^u$

Component *A* ($\mathbf{T}_A$): Eq. (11), (12) with $E_1' = 0$

Component *B* ($\mathbf{T}_B$): Eq. (16), (17)

Component *C* ($\mathbf{T}_C$): Eq. (6) with $C_2' = 0$, (7), (8), (9), (10)

The material properties required to model the untreated and chemically-treated PVC geosynthetics are determined from uniaxial tests. The experiments were conducted at strain-rates of $\dot{\varepsilon}_0 = 4\%/\min$ and $\dot{\varepsilon}_0 = 40\%/\min$ with a peak strain of 140% , followed by unloading. The specific material parameters applicable for untreated PVC material are as follows:

$$\begin{aligned} &C_1 \approx 0.23\,\text{MPa}; \qquad C_2 \approx 0.53\,\text{MPa}; \\ &\kappa_1 = \kappa_2 = \kappa \approx 0.13; \quad \dot{\gamma}_c \approx 5.67\times10^{-7}\,\text{sec}^{-1}; \\ &q \approx 2.0\,\text{MPa}; \quad s \approx 0; \quad E_2' \approx 0.5\,\text{MPa} \end{aligned} \tag{19}$$

Similarly, the constitutive parameters applicable to the chemically-treated material are summarized below:

$$\begin{aligned} &C_1 \approx 9.0\,\text{MPa}; \quad \kappa_1 \approx 12.6; \quad \dot{\gamma}_c \approx 5.6\times10^{-7}\,\text{sec}^{-1} \\ &q \approx 2.64\,\text{MPa}; \quad s \approx 0.1; \quad \dot{\gamma}_c^v \approx 3.2\times10^{-10}\,\text{sec}^{-1}; \\ &\kappa_y = \kappa \approx 0.13; \quad E_y \approx 1.13\,\text{MPa}; \quad E_2 \approx 1.2\,\text{MPa} \end{aligned} \tag{20}$$

4. MEMBRANE INDENTATION EXPERIMENTS

The membrane indentation test facility shown in Figure 4 is designed to apply a controlled movement (Δ) to a rigid spherical indenter (with a diameter $50.8\,\text{mm}$) that interacts with a membrane fixed along a circular boundary. All tests were conducted on PVC specimens that had been exposed to ethanol for a period of 9 months. The rate of indentation $\dot{\Delta}$ is set constant during a test. The test facility has provisions for securing a plane membrane specimen in a fixed condition along a circular boundary of diameter $250\,mm$ (see Figure 4b). The fixed boundary condition is achieved by clamping of the PVC specimen between two aluminium plates ($5\,\text{mm}$ in thickness) using eight $4\,\text{mm}$ screws. To reduce the possibility of slippage at the clamped boundary, a rubber sheet of thickness $3mm$ with an opening of diameter $250\,\text{mm}$ was bonded to the PVC specimen, using a non-reactive instant adhesive.

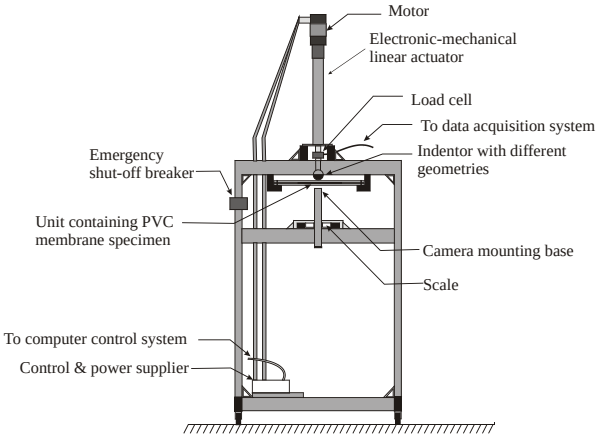

(a) Schematic view of the test frame

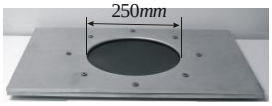

(b) Clamped plate assembly

Figure 4 Apparatus used for membrane indentation tests

During axisymmetric indentation, the contacts were initiated at the center of the circular membrane (Figure 5a). The indentation response was prescribed through the application of the indentation displacement in an incremental manner up to a maximum displacement of $\Delta_{\max} = 50.8\,\text{mm}$. During axisymmetric loading of the chemically-treated PVC, the ratio of the maximum axial displacement to the membrane diameter reached approximately 0.20. This corresponds to a maximum strain of 8% in the radial direction. The load (*P*)-indenter displacement (Δ) response during axisymmetric indentation and the displaced profiles of the membrane are shown in Figure 5a.

The results show a good repeatability between the sets of experiments. The visual images of the deflected shapes were recorded using a high precision (5 Mega pixels) digital camera, which was positioned $1.5m$ from the test specimen. The digital camera was mounted on the test frame in such a way that the image plane was parallel to the plane of the symmetry of the indentation of the membrane. The chemically-treated PVC material exhibited pronounced irreversible deformations after a loading-unloading cycle. During asymmetric indentation, the contacts were initiated at a distance of $42mm$ from the central axis of the circular membrane

(Figure 5b) The indentation responses were examined up to a maximum displacement of $\Delta_{\max} = 38.1mm$, which gave rise to a maximum strain of approximately 10%. In comparison to the case of the axisymmetric indentation, larger forces are needed to induce the same indentation displacement (Figure 8b).

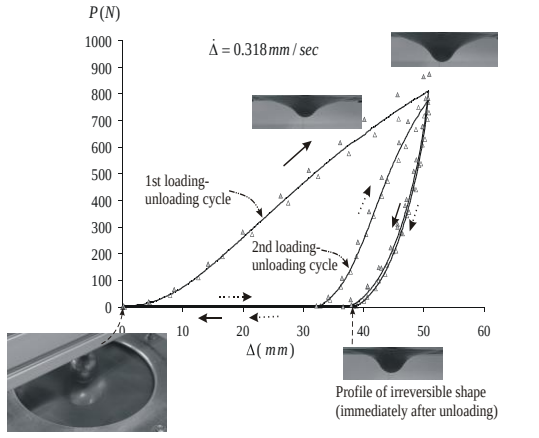

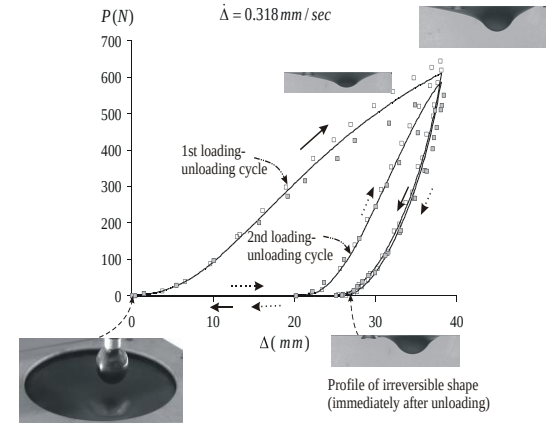

Figure 5 Load-displacement responses of the treated PVC membrane (exposed to pure ethanol for 9 months): (a) subjected to axisymmetric indentation and (b) asymmetric indentation (symbols represent experimental scatter)

5. COMPUTATIONAL MODELLING

The constitutive models for both untreated and chemically-treated polymeric materials can be implemented in computational approaches to examine the mechanical behaviour. In this research program attention focused on membranes that were fixed along a circular boundary and subjected to axisymmetric and asymmetric indentation using a spherical rigid indenter. The computational code used for this purpose was the general purpose finite element code ABAQUS/ Standard™ and the material sub-routine U-MAT was used to implement the constitutive relationships within the computational algorithm. The computational modelling takes into account the rate-sensitive constitutive models and frictional contact between the spherical indenter and the PVC membrane (See also Yu and Selvadurai, 2005, 2007; Selvadurai and Yu, 2005; 2006a, b, 2008). In the nonlinear analysis of frictional contact performed using the ABAQUS™ code, each step is divided into iteration increments. The size of the displacement increment is first chosen and the ABAQUS/Standard™ code automatically assigns the size of subsequent increments. During each increment, the code employs a Newton–Raphson algorithm to perform the iterations and the equilibrium is determined through consideration of the principle of virtual work. The ABAQUS/ Standard™ further utilizes a Backward-Euler scheme as a default finite difference scheme to update variables. Those variables determined from previous iterations that do not change during the iteration between $[t, t+dt]$ can be defined as state variables. The state variables adopted in the analysis include the components of the irreversible deformation gradient $\mathbf{F}^u$ at time *t* and the stress tensors at time *t* in the visco-plastic component included in models *A* and *B*. When a fully backward-Euler finite difference scheme in time is implemented, the updating of γ_0 requires information on the material configuration at $t+dt$. The updated value of γ_0 will have a direct influence on the elasticity parameters for the component *C* in the chosen constitutive model, with the result that the computations will exhibit non-convergence.

The value of γ_0 is thus assumed to remain unchanged during iterations and is taken as a further state variable. For the problems examined here, the PVC membrane only experiences incremental loading during the initial stage where irreversible deformations are absent; the initial values of the state variables can, therefore, be obtained by treating the material as fully elastic. The state variables are updated only when the iteration converges. Both a quadratic triangular membrane element (3M6) and a linear solid triangular prism element (C3D6) were used in the computational modelling. The results indicated no noticeable differences between the two types of elements. The computations presented in the paper were developed using the solid triangular prism element. Figure 6 shows the mesh discretization used in the computational simulation of the axisymmetric indentation problem for the circular membrane. Figure 7 illustrates the comparison of deflection profiles during loading and unloading of an as supplied membrane obtained from the experiments and the computational simulations.

Corresponding results for the asymmetric indentation of the edge supported, as supplied circular membrane are shown in Figures 8 and 9. Further details of the computational procedures and results of comparisons between computational estimates and experimental results can be found in Selvadurai and Yu (2006, 2008) and Yu and Selvadurai (2007).

6. CONTAMINANT LEAKAGE

From a geoenvironmental perspective, it is prudent to assume that some form of a defect can materialize in the geosynthetic liner as result of defective installation, puncturing due to sharp objects in the landfill, burrowing actions of rodents or the effects of localized chemical action and subsequent in-plane stressing of an anchored geosynthetic membrane during landfill loading. In relation to the topic of ethanol exposure, the region of the membrane that will be exposed to ethanol will be stiffer than the unexposed region of the membrane. This contrast in stiffness creates the ideal condition to generate a stress-raiser effect and during in-plane stretching of the membrane by settlement of the subsoils beneath the landfill the geosynthetic membrane can experience rupture forming a crack or defect through which the leachate can escape to the groundwater regime. In such situations the focus will shift to the estimation of the leakage of the leachate from the stored waste to the groundwater. Admittedly, intact secondary clay barriers can be present on either side of the geosynthetic membrane but as indicated, we consider here the worst case scenario where the landfill is directly in contact with the geosynthetic membrane, which in turn is in direct contact with the subsoil. The problem of estimation of leakage from the landfill to the underlying soils can be formulated as a Darcy flow problem between two permeable regions (i.e. the landfill and the underlying soil region separated by an impermeable barrier containing an in-plane two-dimensional defect. Figure 10 shows a typical configuration of the geometry through the defect in the liner and the landfill and subsoil regions. For the development of a convenient analytical result, however, we assume that both the landfill region and the underlying

soils are of large extent compared to the dimensions of the defect in the liner.

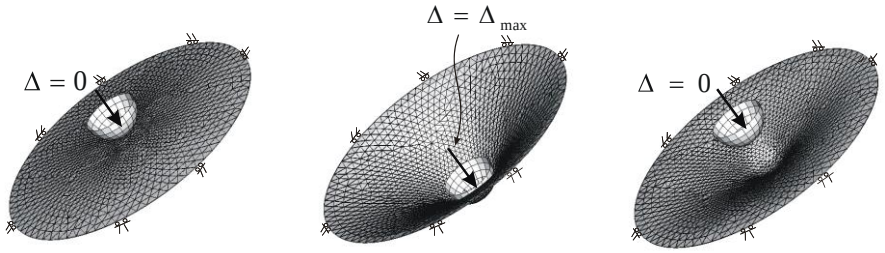

(a) Mesh configuration and boundary conditions (total number of elements: 2086)

(b) Deformed shape during maximum indentation

(c) Irreversible shape after a loading-unloading cycle

Figure 6 Computational simulations of the untreated PVC membrane-symmetric indentation

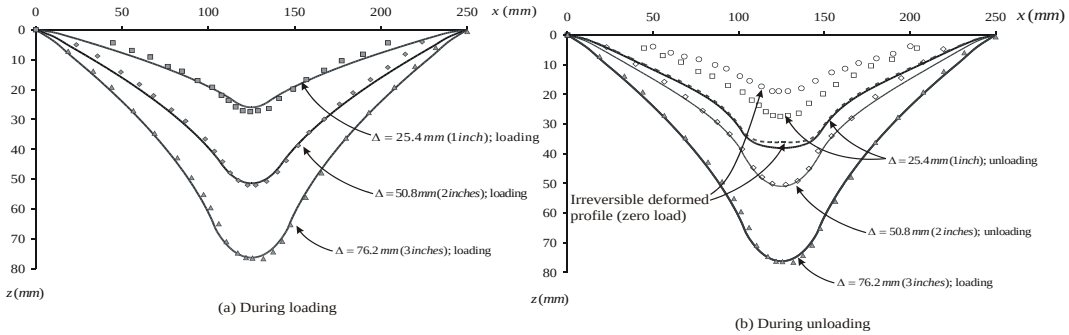

Figure 7 Deflected shapes of untreated membrane during symmetric loading and unloading

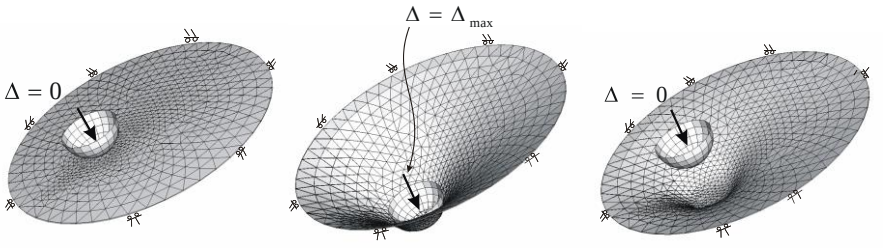

(a) Mesh configuration and boundary conditions (Total number of elements: 1246)

(b) Deformed shape during maximum indentation

(c) Irreversible shape after a loading-unloading cycle

Figure 8 Computational simulations of the untreated PVC membrane-non-symmetric indentation

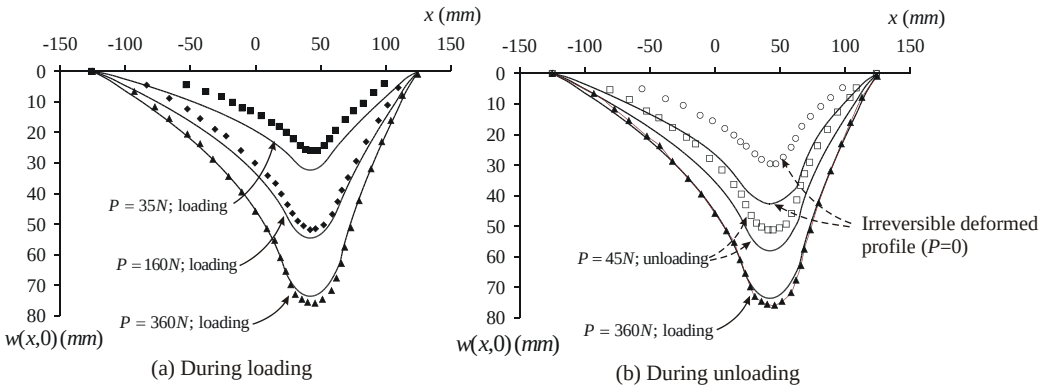

Figure 9 Deflected shapes of untreated membrane during asymmetric loading and unloading

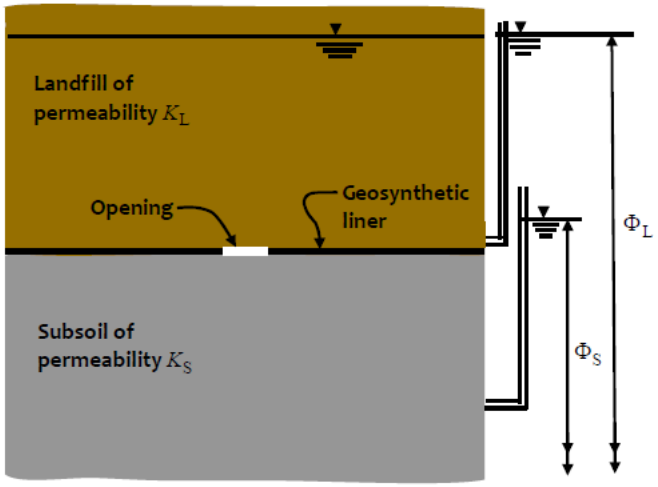

Figure 10 Defect in a geosynthetic liner separating a landfill region from the subsoils

We consider a bi-material porous region that contains a plane impermeable geosynthetic barrier at the interface of the two porous media and fluid leakage occurs through an elliptical defect in the barrier (Figure 11). The fluid flow characteristics are governed by Darcy's law and the permeabilities are defined by K_L (the landfill region) and K_S (the subsoil region). The reduced Bernoulli potential associated with Darcy flow is defined by $\Phi(\mathbf{x})$ and this neglects the velocity potential. The datum is taken as a suitable plane and we assume that the regions L and S are subjected, respectively, to non-interacting far-field reduced Bernoulli potentials Φ_L and Φ_S respectively, with $\Phi_L > \Phi_S$. For purposes of model development, we assume that the non-deformable dissimilar porous region shown in Figure 11 contains fluids with similar properties, although it should be noted that the viscosity and other properties of the contaminating leachates can be different from that of groundwater. In order to develop a convenient analytical result that can be used to estimate the steady fluid leakage through the crack, we shall adopt this assumption. It can be shown that for isochoric Darcy flow in an isotropic non-deformable porous medium the mass conservation law gives $\nabla.\mathbf{v} = 0$, where $\mathbf{v}(\mathbf{x})$ is the velocity vector and $\mathbf{x}$ is the spatial coordinate.

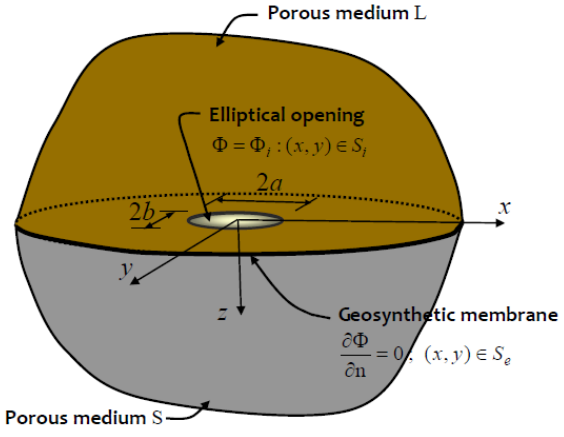

Figure 11 Elliptical opening in the geosynthetic membrane at the interface between the landfill and the subsoil

For an isotropic porous medium, Darcy's law can be written as

$$\mathbf{v}(\mathbf{x}) = -\frac{K\gamma_w}{\mu}\nabla\Phi \tag{21}$$

where K is the permeability, γ_w is the unit weight of the fluid and μ is its dynamic viscosity. Combining Darcy's law and the fluid mass conservation principle, we obtain the partial differential equation governing $\Phi(\mathbf{x})$ as

$$\nabla^2\Phi(\mathbf{x}) = 0 \tag{22}$$

where ∇^2 is Laplace's operator. We consider the mixed boundary value problem in potential theory referred to a half space region, the boundary of which is subject to the relevant Dirichlet and Neumann boundary conditions applicable to an impermeable region with an elliptical opening. The planar region corresponding to the elliptical defect (S_i) and the region exterior to the defect (S_e) are defined as follows:

$$\left(\frac{x}{a}\right)^2 + \left(\frac{y}{b}\right)^2 \le 1 \ ; \ S_i \quad ; \quad \left(\frac{x}{a}\right)^2 + \left(\frac{y}{b}\right)^2 > 1 \ ; \ S_e \tag{23}$$

where a and b are, respectively, the semi-major and the semi-minor axes of the elliptical region. We consider the mixed boundary value problem in potential theory referred to the elliptical aperture such that

$$(\Phi)_{z=0} = \Phi_i = \text{const.} \ ; \ (x,y) \in S_i \tag{24}$$

$$\left(\frac{\partial\Phi}{\partial z}\right)_{z=0} = 0 \ ; \ (x,y) \in S_e \tag{25}$$

where Φ_i is the constant Bernoulli potential over the elliptical interior region, which is dictated by the constant pressure potential over this region and the datum is taken as the plane of the defect. Since the problem examined has a three-dimensional configuration, the regularity conditions applicable to a semi-infinite domain should also be satisfied. In this case the far-field potential in the region L is Φ_L. For the solution of the mixed boundary value problem posed by (24) and (25) we assume, however, that the potential $\Phi(\mathbf{x})$ decays uniformly to zero as $\mathbf{x} \to \infty$. Since the Bernoulli potential is indeterminate to within an arbitrary constant, the far-field value can be added to satisfy the value of the constant potential regularity condition as $\mathbf{x} \to \infty$. The solution to the mixed boundary value problem in potential theory, governed by the partial differential equation (22) and mixed boundary conditions (24) and (25), can be developed in a variety of ways, the most widely accepted being the formulation that employs a generalized ellipsoidal coordinate system and by developing the solution to the opening with an elliptical plan form as a limiting case of an ellipsoid. This approach was used by Lamb (1927) to develop a solution for the motion of a perfect fluid through an elliptical aperture. The result can also be developed using the formal developments in potential theory given by Morse and Feshbach (1953). Similar developments have been used by Green and Sneddon (1950), Kassir and Sih (1968), Walpole (1991) and Selvadurai (1982) in developing canonical results for elliptical cracks and elliptical inclusions embedded in isotropic and transversely

isotropic elastic solids. The solution can be most conveniently formulated in relation to a set of ellipsoidal coordinates (ξ,η,ζ) of the point (x, y, z), which are the roots of the cubic equation in θ defined by

$$\frac{x^2}{(a^2+\theta)}+\frac{y^2}{(b^2+\theta)}+\frac{z^2}{\theta}-1=0 \tag{26}$$

The ellipsoidal coordinate system (ξ,η,ζ) chosen ensures that the interior Dirichlet region S_i corresponds to the ellipse $\xi=0$ and the exterior Neumann region S_e corresponds to a hyperboloid of one sheet $\eta=0$. The mixed boundary conditions (24) and (25) can be explicitly satisfied by the harmonic function

$$\Phi(x,y,z)=\frac{a\,\Phi_i}{\mathrm{K}(\sigma)}\int_{\xi}^{\infty}\frac{ds}{\sqrt{s(a^2+s)(b^2+s)}} \tag{27}$$

where

$$\xi=a^2(\mathrm{sn}^{-2}u-1) \tag{28}$$

and $\mathrm{sn}u$ represents the Jacobian elliptic function defined by

$$\int_0^{\mathrm{sn}(u,\sigma)}\frac{dt}{\sqrt{(1-t^2)(1-\sigma^2t^2)}}=(u,\sigma) \tag{29}$$

In a numerical evaluation of $\mathrm{sn}u$, it is convenient to express the function in the series form

$$\mathrm{sn}(u,\sigma)=u-(1+\sigma^2)\frac{u^3}{3!}+(1+14\sigma^2+\sigma^4)\frac{u^5}{5!} \tag{30}$$
$$-(1+135\sigma^2+135\sigma^4+\sigma^6)\frac{u^7}{7!}+\ldots$$

The complete elliptic integral of the first-kind $\mathrm{K}(\sigma)$ is defined by

$$\mathrm{K}(\sigma)=\int_0^{\pi/2}\frac{d\varsigma}{\sqrt{1-\sigma^2\sin^2\varsigma}}\quad;\quad\sigma=\left(\frac{a^2-b^2}{a^2}\right)^{1/2} \tag{31}$$

We can generalize the result (27) to account for the effect of the far-field potential $\Phi_{\mathrm{L}}(>\Phi_i)$ and this involves simply changing the potential Φ_i in (27) to $(\Phi_{\mathrm{L}}-\Phi_i)$. The fluid velocity at the elliptical aperture associated with the region L is now given by

$$v_z^{(1)}(x,y,0)=-\frac{K_{\mathrm{L}}\gamma_w}{\mu}\left(\frac{\partial\Phi}{\partial z}\right)_{z=0} \tag{32}$$
$$=\frac{K_{\mathrm{L}}\gamma_w(\Phi_{\mathrm{L}}-\Phi_i)}{b\mu\,\mathrm{K}(\sigma)}\frac{1}{\sqrt{1-\frac{x^2}{a^2}-\frac{y^2}{b^2}}}\quad;\quad(x,y)\in S_i$$

where K_{L} is the permeability of the landfill region. The flow rate out of the elliptical aperture is given by

$$Q=\frac{K_{\mathrm{L}}\gamma_w(\Phi_{\mathrm{L}}-\Phi_i)}{\mu b\,\mathrm{K}(\sigma)}\iint_{S_i}\frac{dx\,dy}{\sqrt{1-\frac{x^2}{a^2}-\frac{y^2}{b^2}}} \tag{33}$$
$$=\frac{2\pi a(\Phi_{\mathrm{L}}-\Phi_i)\gamma_w K_{\mathrm{L}}}{\mu\mathrm{K}(\sigma)}$$

A similar result can be developed for the potential flow problem where flow takes place from the porous halfspace subsoil region at a far field potential $\Phi_{\mathrm{S}}(<\Phi_i)$, which gives the velocity field in the interface approached from subsoil region *S* as

$$v_z^{(2)}(x,y,0)=-\frac{K_{\mathrm{S}}\gamma_w}{\mu}\left(\frac{\partial\Phi}{\partial z}\right)_{z=0}=\frac{K_{\mathrm{S}}\gamma_w(\Phi_i-\Phi_{\mathrm{S}})}{b\mu\,\mathrm{K}(\sigma)}\frac{1}{\sqrt{1-\frac{x^2}{a^2}-\frac{y^2}{b^2}}}\quad;\quad(x,y)\in S_i \tag{34}$$

and the flow rate into the subsoil region is given by

$$Q=\frac{2\pi a(\Phi_i-\Phi_{\mathrm{S}})\gamma_w K_{\mathrm{S}}}{\mu\mathrm{K}(\sigma)} \tag{35}$$

The value of the interface potential Φ_i can be obtained, ensuring continuity of the velocity field at the interface: i.e.

$$v_z^{(\mathrm{L})}(x,y,0)=v_z^{(\mathrm{S})}(x,y,0) \tag{36}$$

which gives, $\Phi_i=(K_{\mathrm{L}}\Phi_{\mathrm{L}}+K_{\mathrm{S}}\Phi_{\mathrm{S}})/(K_{\mathrm{L}}+K_{\mathrm{S}})$. The leakage rate through the elliptical aperture can now be obtained by eliminating Φ_i in either (33) or (35), which gives

$$Q=\frac{2\pi a(\Phi_{\mathrm{L}}-\Phi_{\mathrm{S}})\gamma_w K_{\mathrm{L}}K_{\mathrm{S}}}{\mu(K_{\mathrm{L}}+K_{\mathrm{S}})\mathrm{K}(\sigma)} \tag{37}$$

It is important to note that the result (37) is the exact closed form solution for the steady leakage of an incompressible fluid through an elliptical cavity located at the impermeable geosynthetic separating isotropic non-deformable porous landfill and subsoil regions of dissimilar permeability. The potential problem that is solved satisfies the governing equations of potential flow, the mixed boundary conditions applicable to the potential problem and continuity of both the potential and the flow velocity at the interface where Dirichlet conditions are prescribed. From the uniqueness theorem applicable to mixed boundary value problems in potential theory, this solution is unique (Stakgold (1968), Selvadurai (2000a,b)). It should be noted that the solution is identical even if a continuity of total flux boundary condition is imposed on the interface rather than a continuity of flow velocity. It is noted from (32) and (34) that although the velocity at the boundary of the elliptical defect in the landfill liner is singular, the volume flow rate to the elliptical cavity region is, however, finite. In the special case when the permeability characteristics of one region becomes large (e.g. $K_{\mathrm{S}}\to\infty$), (37) reduces to

$$Q=\frac{2\pi a(\Phi_{\mathrm{L}}-\Phi_{\mathrm{S}})\gamma_w K_{\mathrm{L}}}{\mu\mathrm{K}(\sigma)} \tag{38}$$

For the special case when the elliptical opening has the shape of a circular region of radius *a*, $\mathrm{K}(0)\to\pi/2$ and (38) reduces to the classical result that can be obtained by solving the associated mixed boundary value problem in potential theory for the circular opening at an impervious interface, by appeal to the theory of dual integral equations (Sneddon, 1966). The solution presented for the elliptical defect is valid for all aspect ratios of the defect, which permits the evaluation of leakage rates from narrow cracks. Comparisons of the analytical estimates with computational results are given in Selvadurai (2012, 2014) and the analytical solution provides a benchmark for calibration of computational modelling of the potential problem. It is also worth noting that in instances where the separate porous regions display spatial heterogeneity with a log normal variation in the permeability, which can be characterized by an effective permeability such as the geometric mean (Selvadurai and

Selvadurai, 2010, 2014) the result (37) can be used to estimate the leakage from the elliptical opening.

The result (37) can also be used to estimate or develop bounds for the leakage from a damaged region of arbitrary area A_D, where the bounds for the effective permeability K_D are obtained by considering equivalent elliptical regions that either inscribe or circumscribe the region A_D (Figure 12), i.e.

$$\bar{Q}_I \le \frac{Q\mu}{2\pi\gamma_w(\Phi_L - \Phi_S)\sqrt{A_D K_L K_S}} \le \bar{Q}_C \qquad (39)$$

In (39), $\bar{Q}_n$ $(n = I, C)$ denote the non-dimensional flow rates, which refer to the elliptical regions that either inscribe (I) or circumscribe (C) the region A_D and are given by

$$\bar{Q}_n = \frac{a_n\sqrt{K_L K_S}}{\sqrt{A_D}(K_L + K_S)\mathrm{K}(\sigma_n)} \quad ; \quad (n = I, C) \qquad (40)$$

The non-dimensional presentation is accomplished by ensuring that the bounds correspond to non-dimensional versions derived from (40).

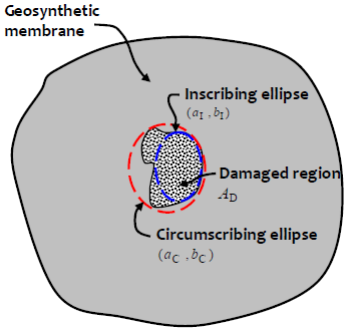

Figure 12 Bounds for the estimation of leakage from an irregular damaged region in a geosynthetic liner

7. CONCLUSIONS

Geosynthetic membranes are used quite extensively for both temporary and permanent protection of the groundwater regime from harmful toxic and hazardous contaminants. The sealing capabilities of geosynthetic barriers can be compromised by exposure of the geosynthetic to chemicals such as acetone and ethanol. The loss of hyperelasticity during exposure to chemicals that can leach out the plasticizer in geosynthetic membranes is a further factor that needs to be accounted for in the analysis and design of the impermeable barriers.

This research summarizes on the development of advanced constitutive models that can account for the loss of hyperelasticity resulting from the removal of the plasticizer. In this study we have presented a unified model that can accommodate the large strain and strain-rate sensitive responses of a PVC membrane in an untreated and chemically-treated state. The validity of the modelling can be assessed either through predictions of uniaxial test results conducted at different strain rates or through predictions of experiments involving three-dimensional deformations of membranes subjected to transverse loading. The latter approach is the more general and requires the implementation of the constitutive models developed in a suitable computational approach. The paper summarizes the results of previous research that involved the implementation of the constitutive models in a general purpose computational code. The computational results accurately predict the response of the transverse deflections of the symmetrically and asymmetrically loaded PVC membranes composed of either untreated or ethanol treated PVC particularly in the loading mode. The irreversible deformations during unloading of both the untreated and ethanol- treated unloading of both the untreated and ethanol-treated circular membranes show that while the trends are accurate, the computational modelling generally underestimates the experimental results. Both the constitutive modelling and the computational approach can be considered as useful for examining the mechanics of hyperelastic rate-sensitive polymeric materials used in geoenvironmental applications.

Although geosynthetic barriers are rarely used as the sole barrier for the containment of leachates from landfills, the potential for exposure of the liner to contaminants can present particularly if heat generated within the decaying landfill can lead to desiccation cracking of the clay liners. In such a situation it is likely that exposure of to the geosynthetic liner to chemicals can lead to loss of plasticity and can contribute to the development of defects that can form a pathway for the contaminant leakage. The paper presents elementary models that can be used to estimate the rate of leakage of fluids from a landfill to the underlying soils. The modelling is approached as a problem of Darcy flow from the permeable landfill to the permeable subsoil. The exact closed form solution based on potential theory can be used to estimate leakage form irregular openings in a geosynthetic liner. The work can also be extended to include advective transport of a contaminant plume leaking from an opening in a defect in a geosynthetic liner.

8. ACKNOWLEDGEMENTS

The work described in this paper was supported by an *NSERC Discovery Grant*, the 2003 *Max Planck Research Prize in the Engineering Sciences* awarded by the Max Planck Gesellschaft, Berlin, Germany and the James McGill Research Chairs program. The author is grateful to Dr. Qifeng Yu for his important contributions to the research work.

9. REFERENCES

Bouazza, A., Zornberg, J.G. and Adam, D. (2002) Geosynthetics in waste containment facilities: recent advances, Geosynthetics-7th International Conference on Geosynthetics, (Delmas, Gourc and Girard, Eds.), 445-506.

Cazzuffi, D. (1987) The use of geomembranes in Italian dams, International Journal of Water Power and dam construction, 26, 44-52.

Contamin, B. and Debeauvais, V. (1998) The Effect of Ethanol Exposure on Burst Strength of a Geomembrane, Research Report, McGill University, Montreal.

Green, A.E. and Adkins, J.E. (1970) Large Elastic Deformations, Oxford University Press, London.

Green, A.E. and Sneddon, I.N. (1950) The distribution of stresses in the neighborhood of a flat elliptical crack in an elastic solid, Proc. Camb. Phil. Soc., 46: 159-163.

Haedrich, T (1995) The Effect of Chemical Exposure on the Burst Strength of a Geomembrane, Master's Thesis, Carleton University, Ottawa.

Kassir, M.K. and Sih, G.C. (1968) Some three-dimensional inclusion problems in elasticity, Int. J. Solids Struct., 4: 225-241

Koerner, R.M. (1998) Designing with Geosynthetics, 4th Edition, Prentice Hall Inc., Upper Saddle River, NJ.

Lamb, H. (1927) Hydrodynamics (6th Ed.), Cambridge University Press, Cambridge.

Lee, E.H. (1969) Elastic-plastic deformation at finite strains, Journal of Applied Mechanics, Transactions of the ASME, 36, 1-6.

Maxwell, J.C. (1892) A Treatise on Elasticity and Magnetism, Clarendon Press, Oxford.

Mooney, M. (1940) A theory of large elastic deformation, Journal of Applied Physics, 11, 583-593.

Morse, P.M. and Feshbach, H. (1953) Methods of Theoretical Physics, Parts I and II, McGraw-Hill, New York

Pezzin, G, Ajroldi, T., Casiraghi, T., Garbuglio, C. and Vittadini, G. (1972) Dynamic-mechanical and tensile properties of poly (vinyl chloride). Influence of thermal history and crystallinity, Journal of Applied Polymer Science, 16, 1839-1849.

Pita, V.J.R.R., Sampaio, E.E.M. and Monteiro, E.E.C. (2002) Mechanical properties evaluation of PVC/plasticizers and PVC/thermoplastic polyurethane blends from extrusion processing, Polymer Testing, 21, 545-550.

Rivlin, R.S. (1948) Large elastic deformations of isotropic materials. IV. Further developments of the general theory. Philosophical Transactions of the Royal Society, A 241, 379-397.

Rivlin, R.S. (1960) Some topics in finite elasticity, Structural Mechanics: Proceedings of the 1st Symposium on Naval Structural Mechanics, (J.N. Goodier & N.J. Hoff, Eds.), 169-198, Pergamon Press, New York.

Rowe, R.K. and Sangam, H.P. (2002) Durability of HDPE geomembranes, Geotextiles and Geomembranes, 20, 77-95.

Selvadurai, A.P.S. (1974) Second-order effects in the torsion of a spherical annular region, International Journal of Engineering Science, 12, 295-310.

Selvadurai, A.P.S. (1975) Distribution of stress in a rubber-like elastic material bounded internally by a rigid spherical inclusion subjected to a central force, Mechanics Research Communications, 2, 99-106.

Selvadurai, A.P.S. (1982) Axial displacement of a rigid elliptical disc inclusion embedded in a transversely isotropic elastic solid, Mech. Res. Comm., 9: 39-45.

Selvadurai, A.P.S. (2000a) Partial Differential Equations in Mechanics, Vol. 1. Fundamentals, Laplace's Equation, Diffusion Equation, Springer-Verlag, Berlin.

Selvadurai, A.P.S. (2000b) Partial Differential Equations in Mechanics, Vol.2. The Biharmonic Equation, Poisson's Equation, Springer-Verlag, Berlin.

Selvadurai, A.P.S. (2002) Second-order elasticity for axisymmetric torsion: a spheroidal coordinates formulation. In Croitoro, E. (Ed.), Proceedings of the 2nd Canadian Conf. on Nonlinear Solid Mechanics, Vancouver, 1, 27-49.

Selvadurai, A.P.S. (2006) Deflections of a rubber membrane, Journal of the Mechanics and Physics of Solids, 54, 1093-1119.

Selvadurai, A.P.S. (2010) On the hydraulic intake shape factor for a circular opening located at an impervious boundary: Influence of inclined stratification, Int. J. Num. Anal. Meth. Geomech., 35: 639-651.

Selvadurai, A.P.S. (2012) Fluid leakage through fractures in an impervious caprock embedded between two geological aquifers, Adv. Water Resour., 41: 76-83.

Selvadurai, A.P.S. (2014) A mixed boundary value problem in potential theory for a bi-material porous region: An application in the environmental geosciences, Mathematics and Mechanics of Complex Systems, 2, 109-122.

Selvadurai, A.P.S. and Selvadurai, P.A. (2010) Surface permeability tests: Experiments and modelling for estimating effective permeability, Proc. Roy. Soc. Ser. A, Math. Phys. Sci., 466: 2819-2846.

Selvadurai, A.P.S. and Shi, M. (2012) Fluid pressure loading of a hyperelastic membrane, International Journal of Non-Linear Mechanics, 47, 228-239.

Selvadurai, A.P.S. and Spencer, A.J.M. (1972) Second order elasticity with axial symmetry. I. General theory, International Journal of Engineering. Science, 10, 97-114.

Selvadurai, A.P.S. and Suvorov, A.P. (2016) Coupled hydro-mechanical effects in a poro-hyperelastic material, Journal of the Mechanics and Physics of Solids, 91, 311-333.

Selvadurai, A.P.S. and Yu, Q. (2005) Mechanics of a discontinuity in a geomaterial, Computers and Geotechnics, 32, 92-106.

Selvadurai, A.P.S. and Yu, Q. (2006a) On the indentation of a polymeric membrane, Proceedings of the Royal Society, Mathematics and Physics Series A, 462, 189-209.

Selvadurai, A.P.S. and Yu, Q. (2006b) Constitutive modelling of a polymeric material subjected to chemical exposure, International Journal of Plasticity, 22, 1089-1122.

Selvadurai, A.P.S. and Yu, Q. (2008) Mechanics of polymeric membranes subjected to chemical exposure, International Journal of Non-Linear Mechanics, 43, 264-276.

Selvadurai, A.P.S., Spencer, A.J.M. and Rudgyard, M.A. (1988) Second order elasticity with axial symmetry. II. Spherical cavity and spherical rigid inclusion problems, International Journal of Engineering Science, 26, 343-360.

Selvadurai, P.A. and Selvadurai, A.P.S. (2014) On the effective permeability of a heterogeneous porous medium: the role of the geometric mean, Philosophical Magazine, 94, 2318-2338.

Sneddon, I.N. (1966) Mixed Boundary Value Problems in Potential Theory, North Holland, Amsterdam.

Spencer, A.J.M. (1970) The static theory of finite elasticity, Journal of the Institute of Mathematics and its Applications, 6,164-200.

Spencer, A.J.M. (2004) Continuum Mechanics, 3rd Ed., Dover Publications, Longman Group, London.

Stakgold, I. (1968) Boundary Value Problems of Mathematical Physics, Vols. I and II, Macmillan, New York.

Suvorov, A.P. and Selvadurai, A.P.S (2016) On poro-hyperelastic shear, Journal of the Mechanics and Physics of Solids, 96, 445-459.

Sweeney, J. and Ward, I.M. (1995) Rate dependent and network phenomena in the multi-axial drawing of poly (vinyl chloride), Polymer, 36, 299-308.

Terzaghi, K. and Lacroix, Y. (1964) Mission Dam: an earth and rockfill dam o n a highly compressible foundation, Geotechnique, 14, 13-50.

Treloar, L.R.G. (1943) Stress-strain data for vulcanized rubber under various types of deformation, Transactions of the Faraday Society, 39, 59-70.

Walpole, L.J. (1991) A translated rigid ellipsoidal inclusion in an elastic medium, Proc. Roy. Soc. Ser. A, 434: 571-585.

Yu, Q. and Selvadurai A.P.S. (2005) Mechanical behaviour of a plasticized PVC membrane subjected to ethanol exposure, Polymer Degradation and Stability, 89, 109-124.

Yu. Q. and Selvadurai, A.P.S. (2007) Mechanics of a rate-dependent polymer network, Philosophical Magazine, 87, 3519-3530.

Zornberg, J.G. & Christopher, B.R. (1999) Geosynthetics. Chapter 27, The Handbook of Groundwater Engineering, Jacques W. Delleur (Editor-in-Chief), CRC Press, Inc., Boca Raton, Florida.